

Fracture mapping for geological prognoses. Comparison of fractures from boreholes, tunnel and 3-D blocks.

M. Zetterlund & L.O. Ericsson

Chalmers University of Technology, Göteborg, Sweden.

M. Stigsson

SKB, Swedish Nuclear Fuel and Waste Management Co., Stockholm, Sweden

Abstract: One of the reasons for uncertainty in geological prognoses is that geological investigations, such as drillings, only represent a small part of the rock mass, and that they may be directionally biased. This study is based on a unique set of data consisting of geological mapping of a tunnel during construction, fracture mapping from three core-drilled boreholes along the tunnel, and fracture mapping of blocks sawed out from a section of the same tunnel. By comparison of the different data sets it is shown how input data to geological models vary depending on what type of fracture mapping it is based on. The study focusses on orientation analysis of fractures using stereographic projection. The results indicate that there are obvious differences in the models due to sampling scale and dimensionality. Yet, the fracture mapping of tunnel faces and boreholes respectively was found to give similar results even though the scanlines along the boreholes are perpendicular to the tunnel faces. The results also indicates that there is a need to improve the detailed conceptual understanding at the tunnel site of the generation and intensity of fracture sets in order to make a reliable interpretation of fracture intensities and orientations.

Theme: Geological Site Characterization

Keywords: Fracture mapping, uncertainties, geological prognoses, Terzaghi correction, stereographic projection.

1 INTRODUCTION

Underground construction projects are always subject to uncertainties relating to geoscientific conditions. One of the reasons for this is that geological investigations, such as drillings, only represent a small part of the rock mass and may be directionally biased. In order to obtain as much and as exact information as possible from drillings, the location and direction of boreholes are of vital importance for the characterization process.

Another type of uncertainty in geological characterization concerns the interpretation of investigation results. Then, conclusions about length, orientations and fracture intensity should be drawn for three dimensional construction problems based on the geology and the geological features of a borehole with a small radius, which is nearly one dimensional. In addition, fracture mapping from different geological investigations, such as outcrops, boreholes, or tunnel walls, gives different prerequisites for interpretation of the fracture network. Interesting parameters are, for example, fracture orientation, size, spatial distribution and intensity.

Efforts have been made to find methods for estimation of mean fracture trace lengths (Kulatilake & Wu 1984, Wu et al. 2011), as well as methods for identification of cluster trends in orientation data (Shanley & Mahtab 1976). By means of Terzaghi correction it is possible to adjust the fracture orientations to reduce bias caused by the sampling orientation (Terzaghi 1965). Mauldon & Mauldon (1997) developed the work of Terzaghi further, with correction factors for boreholes with diameters of up to tunnel scale. The proportional errors of the Terzaghi correction factor and the influence of a blind zone have been mathematically derived by Wang & Mauldon (2006). Davy et al. (2006) presented a development of the correction factor which takes the powerlaw distribution of the fracture radius into account. In all these studies it has been assumed that it is possible to make relevant assumptions about the general fracture geometry based on information from boreholes and mapping of tunnel walls.

Generally, the uncertainties of geological prognoses can be divided into two categories. Firstly, the aleatory uncertainties which are related to the data, including the natural variability of the geological properties for a certain scale, and secondly the epistemic uncertainties which are knowledge based and include uncertainty in models and parameters. This study considers some of the epistemic uncertainties involved in fracture mapping and modeling.

The paper shows how geological models vary depending on what type of fracture mapping the models are based on. The variations can be seen as a measure of the uncertainties that arise during the investigations. Fracture patterns are mainly influenced by two parameters: the orientation of the fractures and their frequencies. Orientations of fractures and fracture sets are based on the state of stress within the rock and the frequencies and spacings of fractures are based on the mechanical properties. Focus in the study is on qualitative orientation analysis of fractures using stereographic projection, and by comparison of the different data sets it is shown how input data to geological models vary depending on what type of investigation the fracture mapping is based on, as well as the scale in which the fractures were mapped.

The study is based on a unique set of data consisting of geological mapping of a tunnel during construction, fracture mapping from three core-drilled boreholes along the tunnel, and fracture mapping of blocks sawed out from a section of the tunnel. The boreholes were part of a pre-investigation program of a tunnel located at Äspö Hard Rock Laboratory (Äspö HRL) in southeast Sweden, and the blocks were sawed out from a section of the same tunnel. The results were benchmarked versus generalized

fracture orientation data bases for the whole rock laboratory facility, at the scale 1- 10 m.

2 BACKGROUND

The geology in the studied area consists mainly of ancient (1.7 Ga) rock types closely related to quartzmonzodiorite and granodiorite, with veins of pegmatite and coarse-grained granite. Alteration, in form of red staining, occurs occasionally, as well as weak alteration in form of epidotization (Hardenby et al. 2008). Most of the identified deformation zones are found in the main rock type. The bedrock has been in brittle mode during approximately 1 Ga and has been subjected to several changes in the state of stress, i.e. both stress difference and orientation of the principal stresses. During the pre-investigations for the Äspö Hard Rock Laboratory more than 3,600 fractures were mapped on outcrops at ground surface and during the construction of the facility approximately 11,000 fractures were mapped (cut off 1 m) in the tunnels and niches. The data have been compiled according to depth intervals (Rhén et al. 1997). The fracture pattern has been interpreted and conceptualized according to a classic Mohr-Coulomb failure criterion with the occurrence of primary vertical conjugate shear planes inclined at acute angles to the axis of maximum compressive stresses during the tectonic evolution. In addition to the dominating vertical fracture sets a predominant horizontal set also occurs (Gustafson 2009). Secondary order fractures may be extensional or in the type of secondary conjugate. At ground surface the primary conjugate vertical fractures have been interpreted to strike 50-75 degrees and around 300 degrees. Secondary order vertical fractures strike N-S and E-W. The horizontal set becomes more assembled versus depth, and at 400-460 m the pattern shows only one pair of conjugate fractures with a predominant peak striking around 300 degrees, see Figure 1.

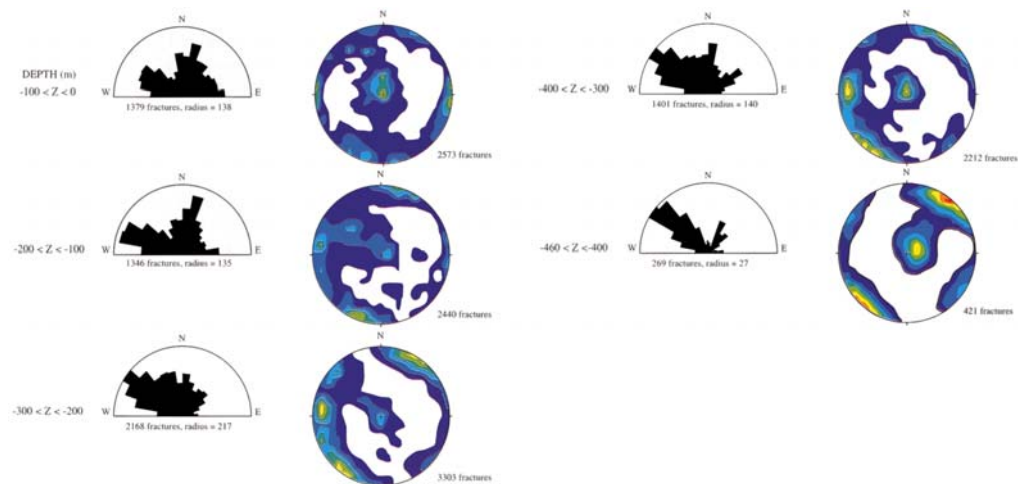


Figure 1. Fracture mappings at different levels at Äspö HRL (modified after Rhén et al. 1997).

The three boreholes, analyzed in this study, were all approximately 100 m long and drilled horizontally in the planned tunnel direction (218 degrees from north) at 450 m depth at Äspö HRL. The location of the boreholes in relation to the tunnel cross-section is shown in Figure 2. A number of geological and hydrogeological investigations were carried out in the boreholes, and detailed geological mapping was performed on all drill cores. During the construction of the tunnel, the floor, roof, and walls of the tunnel, as well as the tunnel face were geologically mapped.

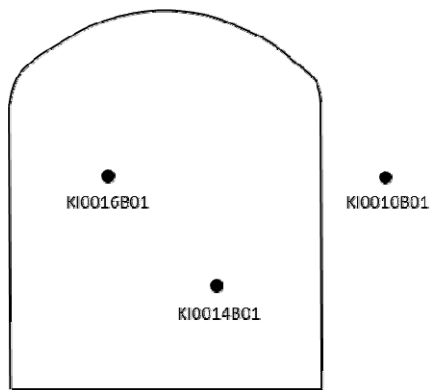


Figure 2. Sketch of boreholes in relation to the tunnel (modified after Hardenby et al. 2008).

From an eight meter long section of the tunnel, eight blocks were excavated from the wall using wire-sawing, see Figure 3a. The blocks were 1 m wide, 1.5 m high and approximately 0.7 m deep. Each block was then sawn into nine or ten slabs, which resulted in a total of 75 slabs, see Figure 3b. Each slab has been cleaned and surveyed, and a total of 2,509 fracture traces in the slabs have been mapped and documented.

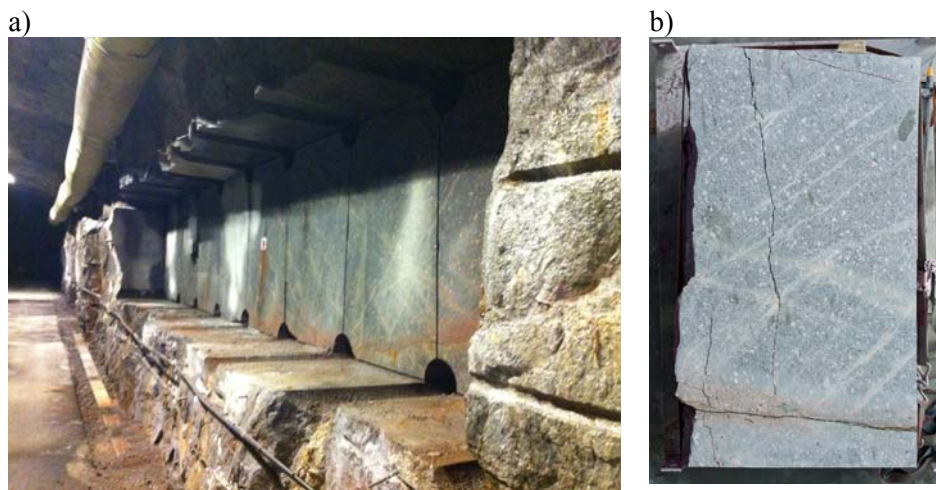


Figure 3. a) Location of excavated blocks in the tunnel (photo: Lars O. Ericsson). b) Example of a slab from one of the blocks (Olsson et al. 2009).

3 DATA SETS

3.1 Boreholes

From the boreholes, fractures from the length sections corresponding to the blocks were selected for analysis; see Table 1. During the mapping of the boreholes the fractures were categorized as open, partly open, or sealed. In the selected length section a total of 246 fractures were mapped in the three boreholes, of which 135 were classified as either open or partly open. Equal area stereographic projections were made of all the fractures together, as well as of the open/partly open fractures separately. In order to reduce the risk of directional bias, all data was Terzaghi corrected. The diameter of the boreholes is 76 mm, which means that it is not possible to draw exact conclusions about the extension of the fractures on a larger scale based on borehole data only.

Table 1. Sections in boreholes corresponding to block section (tunnel length 36-44 m).

Borehole	Section	No. of open/partly open fractures	No. of sealed fractures
KI0010B01	35.30 – 43.30	46	78
KI0014B01	32.68 – 40.68	49	29
KI0016B01	31.30 – 39.30	40	4
Total no of fractures		135	111

3.2 Tunnel

For the tunnel data, the fractures within the length section corresponding to the blocks were selected for analysis. During mapping, the fractures were categorized into four types according to the regular mapping procedure of SKB, see Table 2. Fractures belonging to type 1 and 4 were to be included in the analysis, yet it turned out that no type 1 fractures (truly open natural fractures) had been mapped in the selected tunnel section. The tunnel face data consists of fractures mapped at three different stages of the tunnel excavation, at length 37.5 m, 42.1 m and 45.7 m, including a total of 30 fractures (type 4). The data from the tunnel walls and roof consist of fractures mapped in length section 32.9–48.7 m, 54 fractures (type 4) in total. The cut-off length at mapping was 1 m, and mapped fracture traces could either be seen in the wall or roof only, or they could extend from the walls to the roof.

Table 2. Fracture types in tunnel mapping.

Fracture Type	Description	
1	Open	Truly open natural fracture
2	Tight	Sealed (healed) natural fracture.
3	Ind. Open	Induced fracture which is open due to blasting.
4	Induced/natural open	Natural fracture, formerly healed, which now is more or less open due to blasting.

For the mapping procedure, the tunnel was divided into parts which were mapped in campaigns. The parts consisted of:

- the tunnel wall and roof together,
- the floor of the tunnel, and
- the tunnel face.

3.3 Blocks

The fracture traces of the blocks were classified into three groups: direct blast fractures, blast induced fractures and natural fractures (Olsson et al. 2009). They were then digitalized in Quantum GIS and modeled in a program called Rock Visualisation System (RVS), developed by the Swedish Nuclear Fuel and Waste Management Company (SKB), see Figure 4.

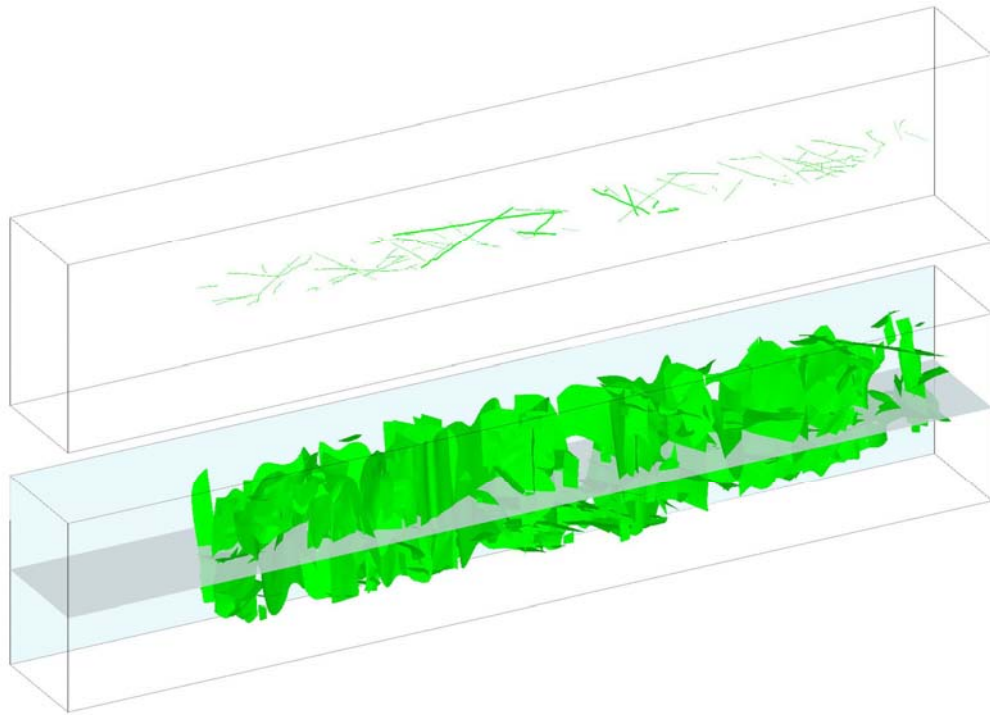


Figure 4. Example of RVS model of the fracture traces mapped in the blocks and classified as natural. The upper box shows fracture traces in the selected cross-section shown in the lower box.

The fractures chosen for analysis in this study were all classified as natural. For the purpose of this study, 424 fractures categorized as natural have been used; out of these approximately 40 percent were classified as healed fractures (Ericsson et al. 2009). The cut off length during mapping was approximately 10 cm and the upper boundary was 8 m in the lengthwise direction of the blocks and 1.5 m in the perpendicular direction.

4 ANALYSIS AND RESULTS

The fracture orientations are visualized in pole plots and contour plots in Lambert equal area nets (Schmidt). When the relative density of the data is of concern, the equal area nets are preferred to equal angle (Wulff) nets, since they preserve the areal relationships. However, whilst preserving the area, they do not preserve the angular relationship of the plotted data (Rowland & Duebendorfer 1994).

The density concentration of data in the contour plots is computed using the Fisher distribution (Fisher, 1953). The distribution is symmetric and when used for asymmetric data it only provides an approximation (Priest 1993), yet it is simple and flexible to use and is known to provide valuable models for fracture data.

The data sets from the boreholes and the mapping of the tunnel face are corrected for orientational bias according to Terzaghi (1965). No correction is made when analyzing the data set consisting of fracture mappings of the tunnel wall together with roof and face, as this data set includes data from three directions. One initial assumption was that the blocks give a fairly realistic three dimensional picture of the fracture network and hence the fractures of the blocks were not corrected for orientational bias.

The Terzaghi correction factor ω of fractures in the boreholes is calculated as:

$$\omega = \frac{1}{\sin \alpha}; 0 \leq \alpha \leq 90$$

where α is the angle between the scanline and the fracture plane, for example, $\alpha = 90$ means a fracture plane perpendicular to the core axis. For tunnel face data, the dihedral angle between the normal of the fracture plane and the normal of the mapping surface is set to α in the calculations of the Terzaghi correction factor.

In the analysis of the boreholes, all data sets are given the same impact on the analysis regardless of the included number of mapped fractures in each borehole. The main reason for this is that the boreholes are drilled fairly close to each other and that they are considered to represent the same rock mass. This is also the case in the analysis of the tunnel face data, where fractures from the three included faces are all given the same weight.

4.1 Boreholes

In Figures 5 and 6, the pole and contour plots of the fractures in the length section of the boreholes corresponding to the blocks are shown. In Figure 5 all mapped fractures are plotted, Figure 6 shows only fractures classified as open or partly open. Both figures show that the fractures are concentrated in three fracture sets, one set striking NW-SE steeply dipping, one set striking approximately 300 degrees and dipping approximately 25 degrees, and one set striking approximately 20 degrees also dipping approximately 25 degrees. When the sealed fractures are excluded, Figure 6, the fractures are more clustered.

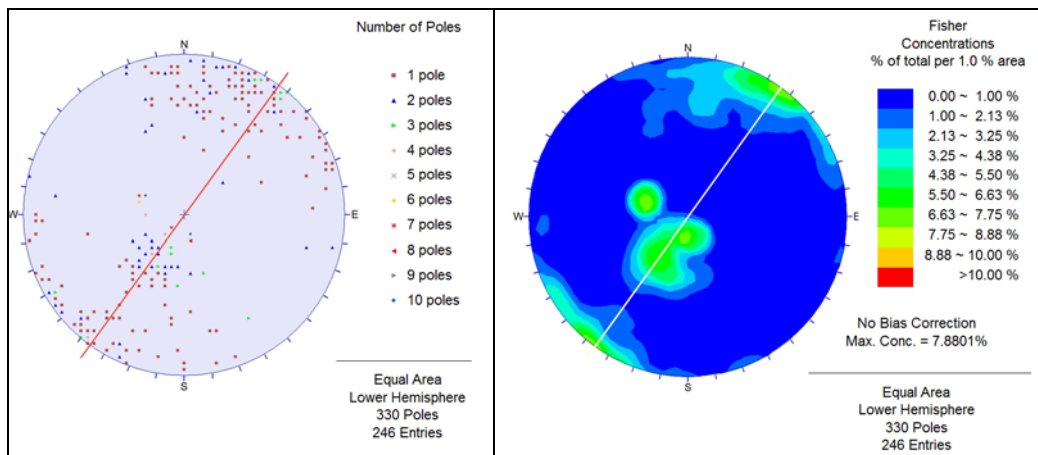


Figure 5. Pole and contour plots (Schmidt nets) of all fractures (open, partly open and sealed) mapped in block sections of boreholes KI0010B01, KI0014B01 and KI0016B01. Terzaghi corrected data.

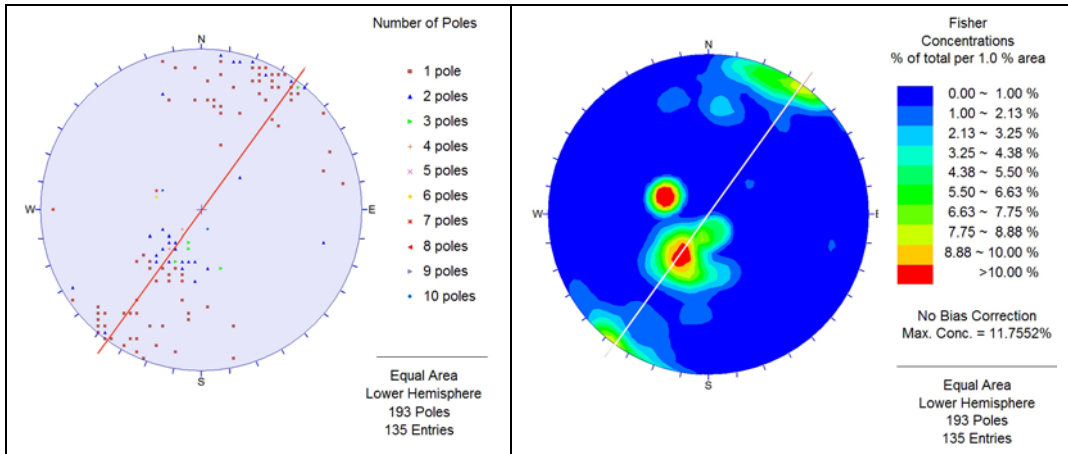


Figure 6. Pole and contour plots (Schmidt nets) of open and partly open fractures mapped in block section of boreholes KI0010B01, KI0014B01 and KI0016B01. Terzaghi corrected data.

The data set from the boreholes was Terzaghi corrected to reduce the bias from the measurement direction. No upper limit was set for the Terzaghi correction factor in the original plots, yet a sensitivity analysis of the impact of the Terzaghi correction was carried out, see Figures 7 and 8, where the maximum value was set to 7 and 10. The figures show that for this data set, the maximum value has a negligible impact since there are so few fractures for which the Terzaghi correction factor is larger than 7.

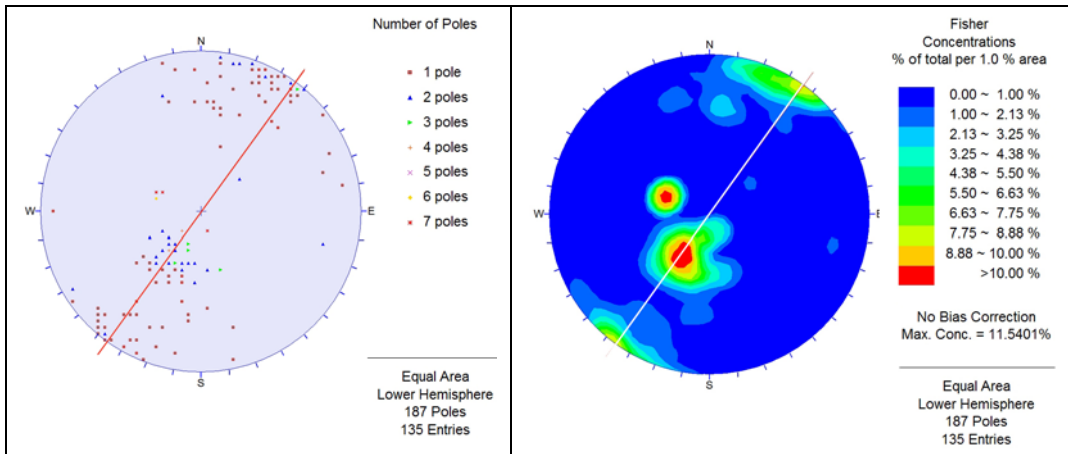


Figure 7. Pole and contour plots (Schmidt nets) of fractures classified as open or partly open in boreholes KI0010B01, KI0014B01 and KI0016B01. Terzaghi corrected data with maximum value 7, corresponding to an α -value of approximately 8.2 degrees.

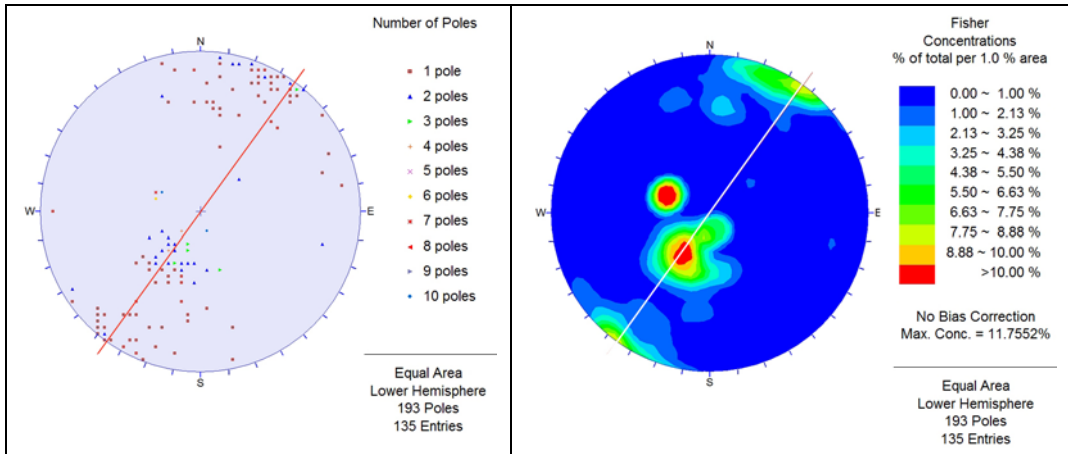


Figure 8. Pole and contour plots (Schmidt nets) of fractures classified as open or partly open in boreholes KI0010B01, KI0014B01 and KI0016B01. Terzaghi corrected data with maximum value 10 corresponding to an α -value of approximately 5.8 degrees.

4.2 Tunnel data

The blocks were sawed out from the tunnel wall at length section 36-44 m; fractures in the corresponding length section of the tunnel were selected and plotted. Figure 9 shows the few fractures mapped in the tunnel faces at length sections 37.5 m, 42.1 m and 45.7 m (mapped area approx. 60 m²). The plots show three fracture sets with not exactly the same, but similar strikes as the sets found in the boreholes, two striking close to the blind spot, WNW-ESE and one set striking 300 degrees and dipping 30 degrees, though different in relative intensity. The fractures were Terzaghi corrected to reduce directional bias with no restriction of the maximum value of the correction factor. Note that the extremely high values of the Fisher concentration are caused by the fact that ten mapped fractures have exactly the same strike and dip.

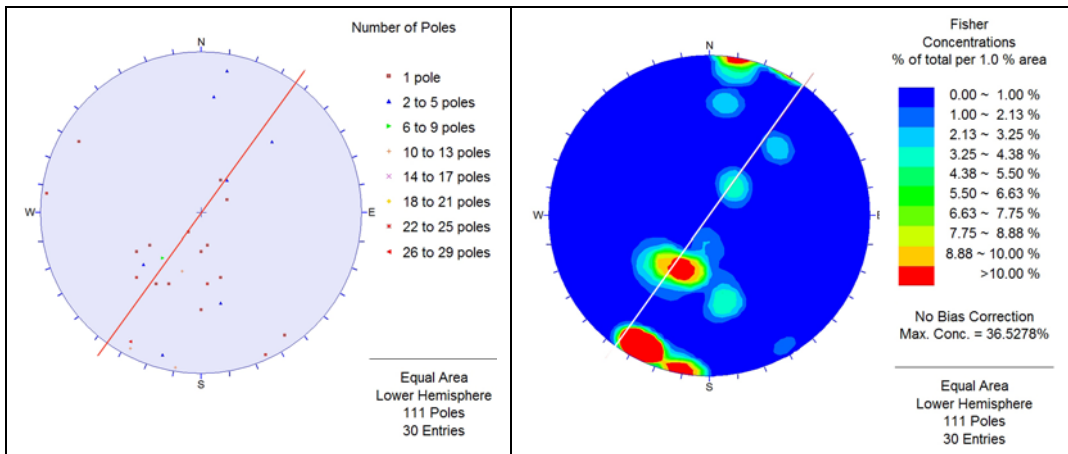


Figure 9. Pole and contour plots (Schmidt nets) of natural fractures mapped in three tunnel faces of section 37.5-45.7m of the TASS tunnel. Terzaghi corrected data.

If the fractures from a longer section of the tunnel than just the section corresponding to the blocks (approx. length 16 m) are plotted, including also the fractures mapped on the tunnel walls (mapped area approx. 117 m²) and roof (mapped area approx. 67 m²), the variation of the fracture orientations is increased, see Figure 10. However, the three fracture sets found from fractures mapped at tunnel face are still the most

distinguished. Note that this data set has not been corrected for orientational bias, since it includes fracture mapping in three directions.

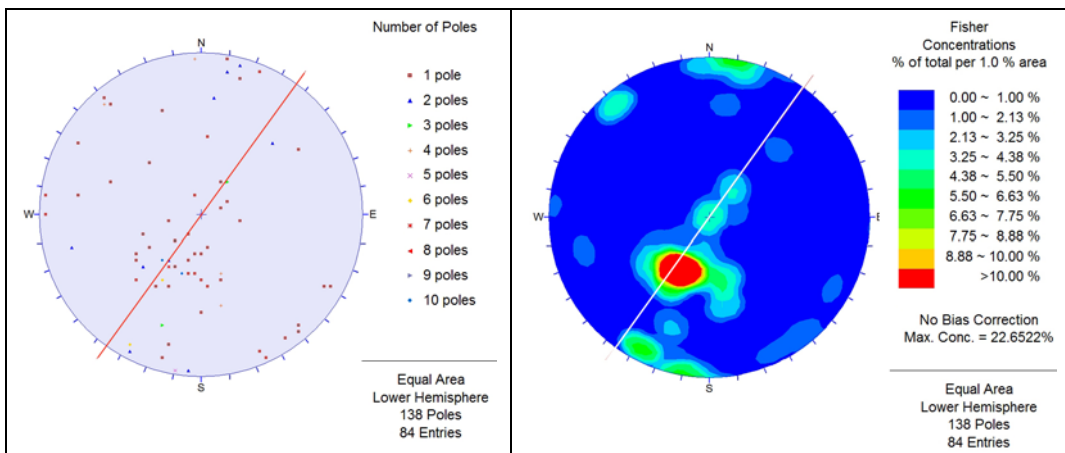


Figure 10. Pole and contour plots (Schmidt nets) of natural fractures mapped in section 32.9-48.7 m of the TASS tunnel. Data includes fractures mapped in tunnel faces, walls and roof. Fracture data has not been Terzaghi corrected for orientational bias.

4.3 Block data

All natural fractures extending over more than one slab from the blocks were classified with higher confidence than fractures whose traces were seen in only one slab. They were plotted without any correction for orientational bias, see Figure 11.

The plots of the fractures mapped on the blocks appear slightly different from the plots of the fractures mapped from the boreholes or in the tunnel. Two main sets are found, one scattered set striking NE-SW and one set with approximate strike/dip of 270/20. A third set, striking WNW-ESE, which was seen in fracture mappings of tunnel and boreholes is barely indicated in the plots of fractures mapped in the blocks. The fractures in the latter set crosses the surface of the slabs at a very small angle and the trace length is commonly only visible in one slab. Hence, they are omitted from the analyses presented in this paper.

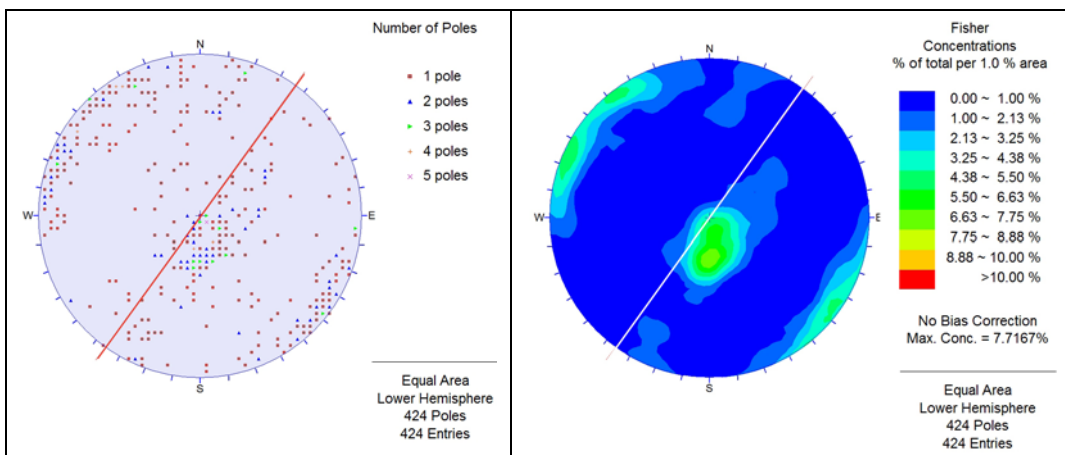


Figure 11. Pole and contour plots (Schmidt nets) of natural fractures mapped in the sawed blocks. Fracture data has not been Terzaghi corrected for orientational bias.

When the natural fractures categorized as healed are excluded from the data, the set striking WNW-ESE from the boreholes appears more distinguished, see Figure 12.

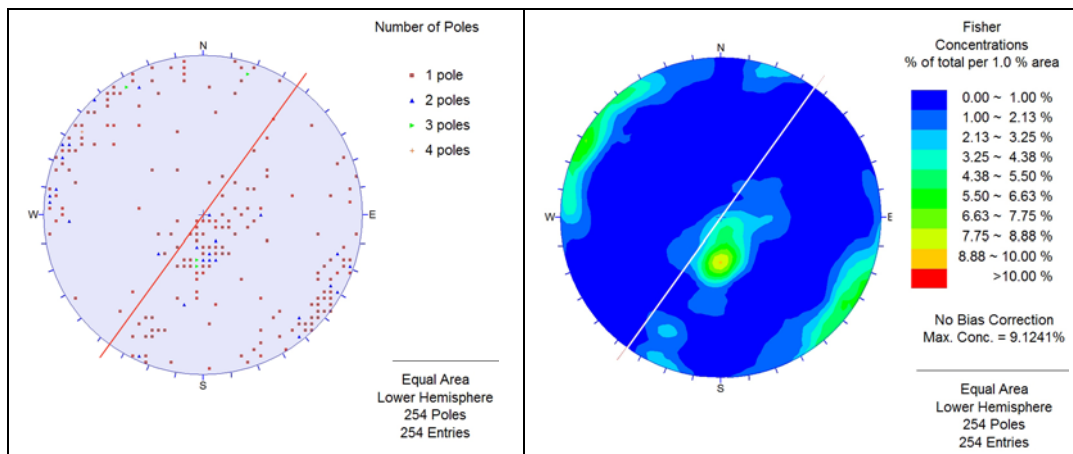


Figure 12. Pole and contour plots (Schmidt nets) of natural fractures mapped as open or tight in the sawed blocks. Fracture data has not been Terzaghi corrected for orientational bias.

5 DISCUSSION AND CONCLUSIONS

In order to get a balanced assessment of fracture orientations the Terzaghi correction factor has been adapted to some of the data bases, i.e. for boreholes and tunnel faces. In literature it is sometimes suggested to assign a maximum value of e.g. 10 to the correction factor (Priest 1993). A sensitivity analysis of the impact of the Terzaghi correction showed that the maximum value has negligible impact since there were few fractures with values of the correction factor larger than 7. The assumption has been that no individual fracture should stand for more than a 5-10 percent of the total number of fractures after Terzaghi correction. Thus the maximum value of the Terzaghi correction factor was not restricted in this study.

The fracture data from the analyzed blocks was initially considered to give the most comprehensive and general picture of the fracture system orientations in the rock mass. However as indicated in the results mentioned above there are obvious differences according to sampling scale and dimensionality.

The scattered fracture set striking NE-SW may be over-represented in the block data. The NE-SW set is not consistent with the fracture set occurrence in the laboratory data (see Figure 1). The relative fracture frequency of this set is higher in the blocks. Seeing that the data is sampled in an only approximately 12 m² rock volume, the scattered orientations do not represent a systematic set according to brittle failure. The over-representation is interpreted as a result of the mapping procedure. The geologist looked at the 'front' of one slab and its sides, and even though the slabs were only 10-15 cm thick, perhaps the resulting model is not three-dimensional as assumed, but should be considered as several parallel surface surveys. In that case, the data set should have been adjusted for orientational bias. Future work may look into this issue to see if fracture data from the blocks can capture all three main fracture sets found in the geological investigations of the tunnel and the laboratory with more reliability in the fracture intensity. Thus the NE-SW fracture set is indicated in the plots of data from the tunnel face, wall and roof, but according to the mapping dimensionality is not seen in the other plots from tunnel and boreholes.

A nearly vertical fracture set striking approximately 110 degrees is vaguely indicated in the plots of block data, but clearly seen in the plots of data from the boreholes, the tunnel face or the plot including the faces, walls and roof. The underestimation of this fracture set in the blocks compared to the data from the whole Äspö HRL in 1996 (Figure 1) is also a matter of mapping dimensionality.

A gently dipping fracture set with approximate strike and dip values of 270 and 20 degrees, respectively, is seen in the plots based on block data. A similar set, but with approximate strike 300 degrees and dip 30 is seen in the plots of the fractures in boreholes and tunnel. Note that the horizontal boreholes identify the fracture set dipping approximately 30 degrees, but do not capture the other fracture set nearly parallel to the boreholes, which is clearly seen in the block data. The Äspö HRL data from 1996 (Figure 1) shows a slightly different general trend of a gently dipping fracture set 20 degrees against SW.

When comparing the plots of tunnel faces and borehole data with plots of fractures mapped in the blocks, it is found that both tunnel face mapping and borehole mapping miss one fracture set identified in block data. Yet, the fracture mapping of tunnel faces identifies nearly the same fracture sets as the boreholes do even though the scanlines along the boreholes are perpendicular to the tunnel faces.

This study focusses on orientation analysis using stereographic projections based on fracture mapping, which are the first basic keys for developing Discrete Fracture Network (DFN) models. Depending on the future usage of a DFN model together with the density and uncertainty of the data, the strategies to develop DFN models may be different. For hydrogeological or rock mechanical purposes, the model will usually consist of a set of statistical parameters, e.g. fracture orientation, size and intensity (Fox et al. 2008, Fox et al. 2007, Munier 2004). It is also possible to use information about stresses, foliation etc. to make more detailed models for these applications, and there are elaborated methods to correct the intensity due to the mapping orientation bias (Wang & Mauldon 2006). However, even though the data base in our case seems comprehensive the interpretation is not straight forward for the purpose of creating a DFN model.

Large epistemic directional uncertainties in the data itself are related to the challenge of understanding the sequence of the geological stress fields that have affected the rock mass over geological time, i.e. the tectonic history (see e.g. Cosgrove 2009). The Baltic shield has been subjected to several tectonic regimes with fractures and zones formed in extensional and shear modes followed by reactivation. This study indicates that there is a need to improve the detailed conceptual understanding at the tunnel site of the generation and intensity of fracture sets in order to make a reliable interpretation of fracture intensities and orientations.

6 ACKNOWLEDGEMENTS

This study was conducted with financial support from the Rock Engineering Research Foundation (BeFo). Data was kindly provided by Swedish Nuclear Fuel and Waste Management Co (SKB). Valuable input from site geologist Oskar Sigurdsson and Ass. Prof Tommy Norberg, Dep. of Mathematical Sciences, Chalmers University of Technology is greatly acknowledged.

7 REFERENCES

- Cosgrove, J.W. (2009). Structural Geology Understanding of Rock Fractures for Improved Rock Mechanics Characterization. *Proceedings from SINOROCK 2009 in Hong Kong, ISRM International Symposium on Rock Mechanics, Rock Characterization, Modelling and Engineering Design Methods*.
- Davy, P., Darcel, C., Bour, O., Munier, R., de Dreuzy, J.R. (2006). A note on the angular correction applied to fracture intensity profiles along drill core. *Journal of Geophysical Research*, 111, B11408, doi:10.29/2005JB004121.

- Ericsson, L.O., Brinkhoff, P., Gustafson, G., Kvartsberg, S. (2009). *Hydraulic Features of the Excavation Disturbed Zone – Laboratory investigations of samples taken from the Q- and S-tunnels at Äspö HRL*. R-09-45. Stockholm. Swedish Nuclear Fuel and Waste Management Co.
- Fisher, R. (1953). Dispersion of a sphere. *Proceedings of the Royal Society of London*, A217, 295-305.
- Fox, A., La Pointe, P., Hermanson, J. and Öhman, J. (2007). *Statistical geological discrete fracture network model. Forsmark modelling stage 2.2*. R-07-46. Stockholm. Swedish Nuclear Fuel and Waste Management Co.
- Fox, A., La Pointe, P., Hermanson, J. and Öhman, J. (2008). *Geological discrete fracture network model for the Laxemar site. Site Descriptive Modelling SDM-Site Laxemar*. R-08-55. Stockholm. Swedish Nuclear Fuel and Waste Management Co.
- Gustafson, G. (2009). *Hydrogeologi för bergbyggare*. Stockholm. Formas T2:2009
- Hardenby, C., Sigurdsson, O., Hernqvist, L. and Bockgård, N. (2008). *Äspö Hard Rock Laboratory. The TASS-tunnel project "Sealing of tunnel at great depth". Geology and hydrogeology - Results from the pre-investigations based in the boreholes KI0010B01, KI0014B01, and KI0016B01*. IPR-08-18. Stockholm. Swedish Nuclear Fuel and Waste Management Co.
- Kulatilake, P. H. S. W. and Wu, T. H. (1984). Estimation of Mean Trace Length of Discontinuities. *Rock Mechanics and Rock Engineering* 17: 215-232.
- Mauldon, M. and Mauldon, J. G. (1997). Fracture Sampling on a Cylinder: From Scanlines to Boreholes and Tunnels. *Rock Mechanics and Rock Engineering* 30(3): 129-144.
- Munier, R. (2004). *Statistical analysis of fracture data, adapted for modelling Discrete Fracture Networks - Version 2*. R-04-06. Stockholm. Swedish Nuclear Fuel and Waste Management Co.
- Olsson, M., Markström, I., Pettersson, A. and Sträng, M. (2009). *Examination of the Excavation Damaged Zone in the TASS tunnel, Äspö HRL*. R-09-39. Stockholm. Swedish Nuclear Fuel and Waste Management Co.
- Priest, S. D. (1993). *Discontinuity Analysis for Rock Engineering*. New York. Chapman & Hall.
- Rhén, I., Gustafson, G., Wikberg, P. (1997). *ÄSPÖ HRL – Geoscientific evaluation 1997/2, Results from pre-investigations and detailed site characterization. Summary report*. SKB TR-97-03. Stockholm. Swedish Nuclear Fuel and Waste Management Co.
- Rowland, S. M. and Duebendorfer, E. M. (1994). *Structural Analysis and Synthesis. A Laboratory Course in Structural Geology*. Boston, Rockwell Scientific Publications.
- Shanley, R. J. and Mahtab, M. A. (1976). Delineation and analysis of Clusters in Orientation Data. *Mathematical Geology* 8(1): 9-23.
- Terzaghi, R. D. (1965). Sources of error in joint surveys. *Geotechnique* 15: 287-304.
- Wang, X. and Mauldon, M. (2006). Proportional errors of the Terzaghi correction factor. *Golden Rocks 2006, The 41st US Symposium on Rock Mechanics (USRMS)*. Golden, CO.
- Wu, Q., Kulatilake, P. H. S. W. and Tang, H.-m. (2011). Comparison of rock discontinuity mean trace length and density estimation methods using discontinuity data from an outcrop in Wenchuan area, China. *Computers and Geotechnics* 38: 258-268.